Reaction Kinetics, Mechanisms and Catalysis (2021) 134:971–987
https://doi.org/10.1007/s11144-021-02106-5

Synthesis of CuO-modified silicon nanowires as a photocatalyst for the degradation of malachite green

Meriem Mahmoudi[1,2,3] · Omar Bouras[1] · Toufik Hadjersi[2] · Michel Baudu[3] · Sihem Aissiou[2]

Received: 1 October 2021 / Accepted: 28 October 2021 / Published online: 5 November 2021

Abstract

This work aims to investigate the malachite green photodegradation by CuO-modified and unmodified silicon nanowires (SiNWs) as photocatalysts in the presence of peroxymonosulfate (PMS) under UV or Visible light irradiations. SiNWs were synthesized by one-step metal assisted-chemical etching of silicon substrate in aqueous ($HF/AgNO_3$) solution and modified with CuO nanoparticles using an electroless deposition technique. The as-prepared samples were characterized by scanning electron microscopy, X-ray diffraction, energy-dispersive X-ray spectroscopy and Fourier transform infrared spectroscopy. Obtained results revealed that the Cu-modified SiNWs exhibit higher photocatalytic activity under both UV and visible irradiations compared to unmodified ones. The addition of PMS to the mixture (photocatalyst/MG) leads to an increase in this activity resulting in almost total discoloration of the order of 98% for an irradiation period of 100 min.

Keywords Silicon nanowires · Cu nanoparticles · Peroxymonosulfate · Photodegradation · Malachite green

Introduction

Water pollution is one of the major environmental concerns produced by anthropogenic activities, originated mostly from industrial, domestic and hospital effluents discharged as wastewaters in various water bodies. Recently, photocatalysis has attracted considerable attention due to its potential application in degrading organic

✉ Michel Baudu
michel.baudu@unilim.fr

[1] Water Environment and Sustainable Development Laboratory, University of Blida-1, Road of Soumaa, PO Box 270, 09000 Blida, Algeria

[2] Semiconductor Technology Research Center for Energetic (CRTSE), 2, Frantz Fanon, Algiers-7 Merveilles, PO Box 140, Algiers, Algeria

[3] PEIRENE EA7500, University of Limoges, 123, Albert Thomas, 87060 Limoges Cedex, France

pollutants in aqueous media [1–3]. For this reason, different photocatalysts have been developed in the degradation of a wide range of contaminants in water. Among them, semiconductors have been most frequently used as photocatalysts due to their wide band gaps [4, 5]. Nanostructured semiconductors such as silicon nanowires (SiNWs) have attracted worldwide research interest due to their numerous properties such as; wide optical absorption range, easy surface modification with metals, organic group and oxides, high specific surface area, stability to the atmospheric environment and low toxicity [1, 2, 5]. These have shown to be equally promising both in photocatalysis applications [6–9] and in other fields such as electronics and photovoltaics [10–13], diagnostic [14], molecular detection [15, 16], batteries [17], binding and detection of viruses [4] and biomedical applications [18]. These new materials are characterized by a one-dimensional structure, which allows them a strong separation of the excited electron–hole pairs. However, the ease of oxidation which gives rise to the formation of silicon oxide (SiO_x) makes them unstable in aqueous solutions. This drawback could never the less be overcome by coating the Si surface with metallic or metal oxide particles. To this end, different nanoscale metals have been anchored on the surface of SiNWs for catalytic purposes, such as Ag [11, 19], Au [1, 3, 19, 20], Pd [3, 19], Pt [3, 19], Cu [2, 21–24], MnO_2 [25], TiO_2 [26]. Among them, copper oxides (CuO and Cu_2O), known as p-type semiconductors with narrow band gaps of 1.2 and 2 eV, respectively, prove to be the most promising materials, since they are characterized by excellent chemical stability, inexpensive, nontoxic and easily implemented [24]. Indeed, they are used in several applications such as catalysis [2, 23, 27], sensors [28], gas sensors [29], optical [30], electrical [31] and solar energy transformation [32–34]. Thus, the modification of the SiNWs with these oxides to produce heterojunctions only has the effect of combining the advantages of these oxides with the high specific surface area of SiNWs and the rapid separation of the photogenerated charge carriers.

Dyes are common water pollutants, widely used in different industries, especially wool, silk, paper, leather and food coloring [35–37]. Among them, malachite green (MG) as a synthetic cationic dye used as a food coloring additive and as dye in wool, paper, leather, cotton and acrylic industries. However, throwing the MG in water system, without prior treatment, can lead to dangerous effect since it can influence the aquatic ecological system due to ecological imbalance. Moreover, it changes the quality of human life and disturbs the food chain [17, 37, 38]. In the literature, there are different reports on the MG degradation. Lavand et al. [35] investigated the degradation of MG by nanoparticles of titanium dioxide co-doped with carbon and iron III under visible light irradiation. Rabie et al. [36] synthesized and studied the efficiency of Nano-ZnO and Co-ZnO supported alagae (sargassum species) in decolorization of MG dye under visible light source. Arslani et al. [37] improved the photocatalytic performance in composing of ZnO with CNTs under Visible light compared to pure ZnO. Mark et al. [38] demonstrated the performance of $CoMn_2O_4$NPs against MG. Hasan et al. [38, 39] synthesized polycrylamide-g-chitosan γ-Fe_2O_3 nanocomposite and studied its utility towards the removal of MG from wastewater. Saad et al. [40] synthesized two types of chitosan-based composites (chitosan/ZnO and chitosan/Ce-ZnO composites) under microwave irradiation as advanced catalysts of enhanced photodegradation activity of MG under visible light. Solis-Casdos

et al. [41] synthesized film photocatalysts from TiO_2 modified with Sn and Eu; the performance of resulting material was demonstrated in photocatalytic degradation using simulated solar light. Hakimyfard et al. [42] demonstrated the performance of synthesized nanostructured doped $As_2Ni_3O_8$ in the degradation of MG in aqueous solution under direct visible light irradiation. Das et al. [43] synthesized $MgFe_2O_4$ as catalyst for the degradation of MG dye. Surendra et al. [44] prepared $ZnFeO_4$nano-photocatalyst for photocatalytic degradation of MG under sunlight and UV irradiations.

The literature report many works on the photocatalytic degradation of malachite green and it was interesting to use this dye as a reference for comparison. Mohameda et al. [45] investigated modified polyacrylonitrile nanofibres/biogenic silica composites for photocatalytic degradation of MG and show the high efficiency of this composite. Cu_2O nanoparticles coat with high surface area can enhance the total effective area of SiNWs for the photochemical reaction, which ameliorates the photocatalytic activity. Moreover, few research works have been carried out on Cu_2O/SiNWs p–n type heterojunction considering the insufficiency of preparation techniques.

In the present work, we electrolessely deposited Cu_2O nanoparticles on SiNWs synthesized by a metal-assisted etching process to make nano-heterojunctions which were experimented to examine their performance in catalytic photodegradation and mineralization of malachite green under UV and Visible light irradiations. A deep characterization of materials was performed for the discussion of their photocatalytic performance.

Thus, the photocatalytic activity of Cu modified SiNWs was investigated with the influence of irradiation time, PMS activation, dye concentration and pH values on the photocatalytic efficiency. In addition, the photocatalytic degradation mechanism of MG was proposed.

Experimental

Materials

Silicon wafers were purchased from Sil'tronix (France). All cleaning and etching chemical reagents of analytical grade used in this study such as hydrogen fluoride (HF,40–45%), oxygen peroxide (H_2O_2, 34.5–36.5%), nitrates of silver ($AgNO_3$, 99.8%), acetone (98%), isopropanol (99.8%), sulfuric acid (H_2SO_4, 95–97%), nitric acid (HNO_3, 69%), potassium sodium tartrate tetrahydrate ($KNaC_4H_4O_6{\cdot}4H_2O$, 99%), copper sulfate pentahydrate ($CuSO_4{\cdot}5H_2O$, 99%),formaldehyde (HCHO, 37%), sodium hydroxide (NaOH), oxone monopersulfate compound (PMS) were purchased from Sigma-Aldrich.

Malachite green MG (C23H25 N2Cl) was purchased from Fluka AG and was used without further purification. The deionized water of resistivity 18.2 MΩ cm was used throughout all the experiments.

Elaboration of SiNWs

Silicon nanowires were elaborated on n-type Si (100) substrate of 1–10 Ω cm resistivity by one-step metal-assisted chemical etching process.

Firstly, the substrates with 1 cm × 1 cm size were degreased in acetone and isopropanol and then cleaned in a piranha solution (H_2SO_4/H_2O_2; 3/1) for 15 min at 80 °C followed by copious rinsing with deionized water and drying under a stream of nitrogen.

After immersing in an aqueous HF (10%) solution to remove the native oxide, rinsing and drying under a stream of dry N_2, the substrates were dipped in an aqueous 5 M HF–0.02 M $AgNO_3$ solution at room temperature for 1 min. The samples with deposited silver nanoparticles were rinsed with deionized water and dried under nitrogen then immersed into a bath containing 5 M HF and 0.4 M H_2O_2 for 60 min to form nanowires. Subsequently, the Si pieces were plunged in concentrated HNO_3 for 3 min to remove all Ag traces, followed by rinsing with deionized water and drying under a stream of nitrogen [3, 25].

Modification of SiNWs

The decoration of SiNWs was performed by a chemical method described by Xiong et al. [22]. Copper nanoparticles were deposited on SiNWs via electroless deposition in alkaline solution. This solution was prepared by adding 50 mL of 0.2 M $KNaC_4H_4O_6{\cdot}4H_2O$ to 100 mL of 0.15 M $CuSO_4{\cdot}5H_2O$ solution under regular magnetic stirring. After a period of 10 min, 5 mL of 1 M HCHO solution was added drop by drop to the mixed solution. Afterwards, NaOH solution (2 M) was added gradually to reach a pH between 12 and 13.5. Obtained mixture was maintained at 45 °C, then, the SiNWs were immersed into it for 10 min. Finally, the samples were rinsed with deionized water and dried under a gentle stream of nitrogen.

Photocatalytic experiments

The photocatalytic performance of Cu-modified SiNWs (SiNWs-Cu) was evaluated through the degradation of MG. A solution of 2.5×10^{-5} M was prepared by dissolving MG powder in deionized water under magnetic stirring at room temperature for 1 h. The samples (1 cm × 1 cm) were immersed into a 5 mL of MG aqueous solution which was irradiated with UV (λ = 350–400 nm) or visible light (λ = 400–700 nm) at room temperature for 100 min. The MG degradation was followed by measuring intensity of its absorption peak at 617 nm with a UV–Vis absorption spectrophotometer every 10 min. The MG solution irradiation was carried out under different conditions:

(a) Direct irradiation without sample (photolysis).
(b) In the presence of SiNWs.

(c) In the presence of SiNWs-Cu.
(d) By adding of oxonemonopersulfate compound (PMS) for each case quoted just before.

All photodegradation processes were carried out after reaching adsorption equilibrium between solid material and MG aqueous solution over 10 min in the dark.

To examine the effect of ionization of MG molecule, the pH value of MG solution was adjusted using a diluted HCl (0.1 M) or diluted NaOH (0.1 M) solutions.

Sample characterization

The morphology of prepared samples was studied employing a secondary electrons mode (SE) using an SEM505 scanning microscope (Phillips), while the crystallinity of the sample was analyzed with a D8ADVANCEX-ray diffractometer (supplied by Bruker corporation from Germany). All diffraction peaks were identified using JCPDS databases. The chemical compositions of samples were analyzed by the energy-dispersive X-ray spectroscopy (EDS). The surface chemistry of the samples was monitored by fourier transform infrared spectroscopy (FTIR). The corresponding FTIR spectra were recorded using a PerkinElmer FT-IR/NIR spectrometer in the 650–4000 cm^{-1} region. The absorption spectra of the malachite green solutions contained in quartz cell with an optical path of 10 mm were recorded using a Varian Cary 50 Probe UV–Vis spectrophotometer in the wavelength range 400–800 nm.

Results and discussion

Characterization of SiNWs

The cross-sectional SEM images of the formed SiNWs supports (Fig. 1A), clearly show that they are vertically aligned to the surface on silicon substrate. The interface between the layer of nanowires (approximately 11 µm in length) and

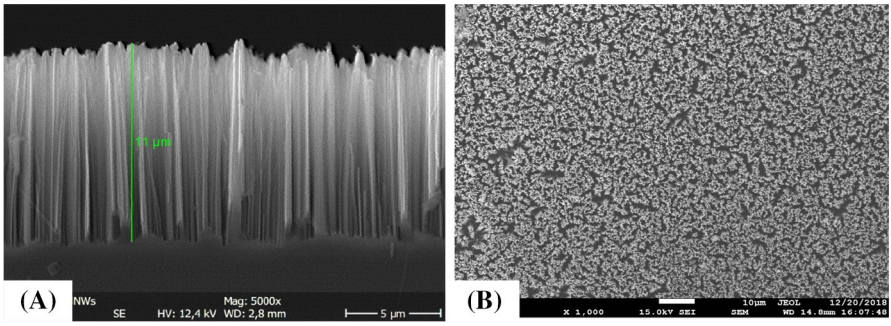

Fig. 1 SEM images of silicon nanowires elaborated by a one-step Ag-assisted chemical etching process, **A** Cross-sectional, **B** plan view

substrate is clearly distinguished thus indicating that the etching was uniform. The plan SEM image shows that the silicon surface was uniformly covered with nanowires. Moreover it can viewed that the nanowire tips adhere together to constitute bundles, this phenomenon is due to Van der Waals forces (Fig. 1A and B) [3].

As shown in (Fig. 2A), the cross section SEM image depicts that the Cu nanoparticles are uniformly deposited onto the sidewalls of SiNWs until the interface SiNWs/silicon substrate (noted by SiNWs-Cu). However, the plan SEM image (Fig. 2B) illustrates that nanoparticles of size lower than 1 µm (approximately between 62 and 312 nm) are deposited on to SiNWs tips. The deposition occurs according to electroless metal deposition process. Indeed, since the electronic activity of copper ions is higher than that of Si, Cu ions capture electrons from silicon uniformly to form a thin copper nanoparticles coat [2].

The EDS data recorded from SiNWs and SiNWs-Cu are shown in (Fig. S1A and S1B). As depicted in (Fig. S1A), the EDS spectrum of the SiNWs shows an intense peak of Si, a lower intensity peak of O and a very low intensity peak of C. This indicates that SiNWs are mainly composed of Si while C and O come from contamination and the native oxide formation on the SiNWs surface, respectively. After modification, a new peak corresponding to Cu appears in the EDS spectrum and a slightly increases of O peak intensity is noted (Fig. S1B) which confirm the deposition of oxidized Cu nanoparticles onto the SiNWs.

To analyze the crystalline structure of SiNWs and Cu- modified SiNWs, XRD measurements were performed. The corresponding XRD patterns of SiNWs and SiNWs-Cu are shown in (Fig. 3A and B). The unmodified SiNWs exhibits a high peak at $2\Theta = 54.87°$ which corresponds to the (311) crystal plane of silicon (Si) (JCPDS card-00-027-1402). The difference between this crystallographic orientation and the initial orientation of silicon substrate (100) is due to the fact that the measurement was made at a grazing angle which allows analyzing only the top part of the nanowires that are tilted [19].

In addition, peaks at $2\Theta = 46.20°$, 83.15°, 97.20° and 98.10° can be assigned to the (023), (311), (214) and (223) planes of SiO_2 according to JCPDS cards (Nos.

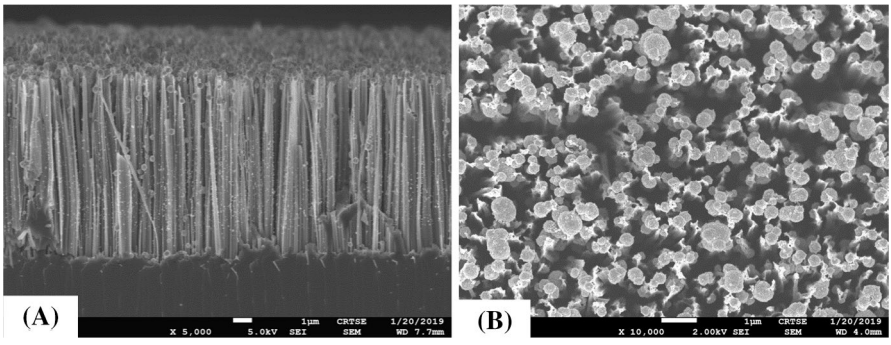

Fig. 2 Cross sectional (**A**) and plan view (**B**) SEM images of silicon nanowires modified with Cu nanoparticles

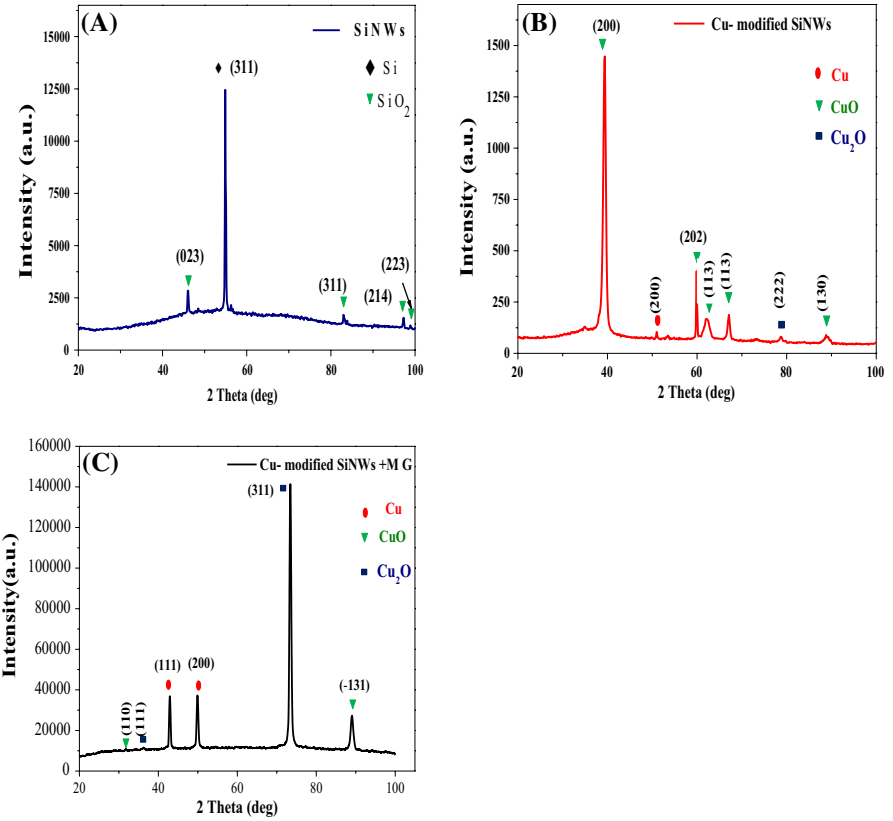

Fig. 3 XRD patterns of unmodified SiNWs (**A**), Cu -modified SiNWs (**B**), Cu-modified SiNWs after MG photodegradation process (**C**); $C_0 = 2.5 \times 10^{-5}$ M, PMS = 0.3 mM

00-046-1045 and 00.027-1402). The intensity of these peaks is low which indicates the formation of native oxide on the surfaces of SiNWs.

As shown in Fig. 3B, a series of characteristic peaks are noticed. The peak at $2\Theta = 50.92°$ corresponds to (200) plane of Cu (JCPDS card-00-004-0836), while the peaks at $2\Theta = 39.52°$, 59.84°, 62.19°, 67.20° and 88.83° are related to the (200), (202), (113), (113)and (130) planes of CuO (JCPDS card-00-048-1548). We can also notice the presence of peak at $2\Theta = 78.69°$ which corresponds to (222) plane of Cu_2O. The formation of CuO and Cu_2O is due to the oxidation of Cu in open air, whereas the absence of Si peak is due to the large amount of deposit copper on upper part of SiNWs as observed by SEM (Fig. 2B). The presence of the two phases Cu_2O and Cu promotes the production of hydroxyl radicals OH·, which are strong oxidizing agents for organic pollutants [19].

The SiNWs-Cu photocatalyst used in MG photodegradation process was also analyzed by XRD (Fig. 3C). We can notice a disappearance of peak at $2\theta = 39.52°$ and diminution of number of peaks corresponding to CuO after the degradation process, and an appearance of a high intensity peak at $2\theta = 73.50°$ and a low

intensity peak at $2\theta = 36.31°$ which corresponds of the (311) and (111) crystal plane of Cu_2O (JCPDS card-00-005-0667). This phase indicates that there is no chemical reaction between photocatalyst and malachite green solution, which means that the photocatalyst is stable.

FTIR measurements were carried out on prepared samples to characterize the changes in the chemical composition of SiNWs after photodegradation of MG dye. The corresponding FTIR spectra of SiNWs and Cu-SiNWs before and after MG photodegradation recorded in transmittance mode in the 400–4500 cm^{-1} spectral range are shown in (Fig. 4).

The strongest broad band peak appearing in the region between 1000 and 1250 cm^{-1} is assigned to the Si–O–Si asymmetric stretching vibrations due to the high oxidation. This band is subdivided into two absorption peaks at 1070 cm^{-1} and 1220 cm^{-1} which are assigned to the transverse optical phonons in thin SiO_x layer and to Si–O stretching mode. Another small band observed at 800 cm^{-1}, curve (c), is assigned to Si–OH bond which is attributed to the oxidation of the surface of Cu modified SiNWs after contact with MG solution. The intense peak at 630 cm^{-1}, curve (c), which can be assigned to Si–O–Si stretching, is due to the oxidation of SiNWs after photodegradation process. Thus, these results clearly show that the samples are oxidized after modification by Cu and photodegradation processes. In addition, there is no appearance of new peaks which could be related to the formation of bonds with MG molecules after photodegradation process. This clearly confirms the absence of surface modification and the stability of the photocatalyst surface.

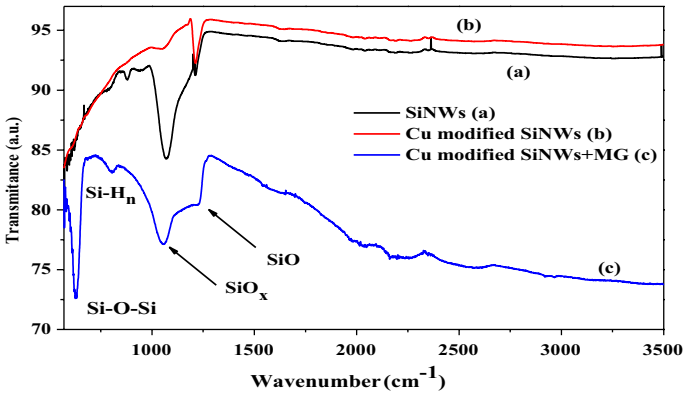

Fig. 4 FTIR spectra of SiNWs (a), Cu-modified SiNWs before photodegradation process (b) and Cu-modified SiNWs after MG photodegradation process (c); $C_0 = 2.5 \times 10^{-5}$ M, PMS = 0.3 mM

Photocatalytic activity

Degradation of MG without irradiation

Raw and modified SiNWs were evaluated for adsorption and oxidation reaction by experiments without irradiation (Fig. S2). The use of SiNWs-Cu and unmodified nanowires as catalysts without irradiation gives close values of the degradation which are about 21 and 17%, respectively.

These very low values can be attributes to the adsorption of MG molecules onto active surface of SiNWs and Cu_2O nanoparticles. It can be seen clearly that the use of PMS alone gives a high degradation rate of about 73% that can be explained by the fact that PMS can be activated by electron transfer from pollutants to PMS which plays a role of an electron acceptor [46]. The use of PMS with modified and unmodified nanowires increases slightly the degradation rate to about 78 and 79%, respectively. This little enhancement can be explained by the activation of PMS by SiNWs or Cu_2O nanoparticles by a nanoradical pathway [46]. These results indicate that the Cu nanoparticles cannot be activated without irradiation.

Degradation of MG under irradiations

Same experiments as before were performed but with visible and UV irradiation. We observe that the photolysis for 100 min of MG under UV and visible light irradiations allow have very low degradation rates which are about 0.62 and 0.15%, respectively.

Dye solutions are firstly examined only with PMS under irradiations. Indeed, adding a very low amount of PMS (7.5 µL), the degradation rates significantly increases to around 68 and 32% under UV and Visible light irradiations, respectively. This enhancement of photodegradation rate (Fig. 5A) is owing to the activation of PMS by ultraviolet irradiations and the electron transfer from MG and water molecules to PMS molecules. In (Fig. 5B), the low enhancement of photodegradation rate, compared to (Fig. 5A), is due probably to the fact that the activation of PMS is made by electron transfer from MG and water molecules to PMS molecules only as was reported in the literature [46–48].

For the photo-degradation, MG molecules must be well adsorbed on the surface of materials. When a MG solution is irradiated with UV or visible light, electron–hole pairs are generated which reacted with water to generate hydroxyl and superoxide radicals, which accelerate the degradation of pollutant. This process explains the high photodegradation rates obtained when SiNWs, which have a high surface to volume ratio, were used: 78.23 and 78.94% for UV and Visible light irradiations, respectively.

Degradation rates as high as 98.69 and 99% were obtained for cases of UV and visible light irradiations, respectively when SiNWs-Cu were used. This trend is obviously noted in (Fig. S3A and S3B) where the absorption peak intensities appreciably decreased.

This is partly due to the large amount of Cu nanoparticles deposited on the SiNWs as shown in the SEM image of (Fig. 2A and B), which gives rise to the

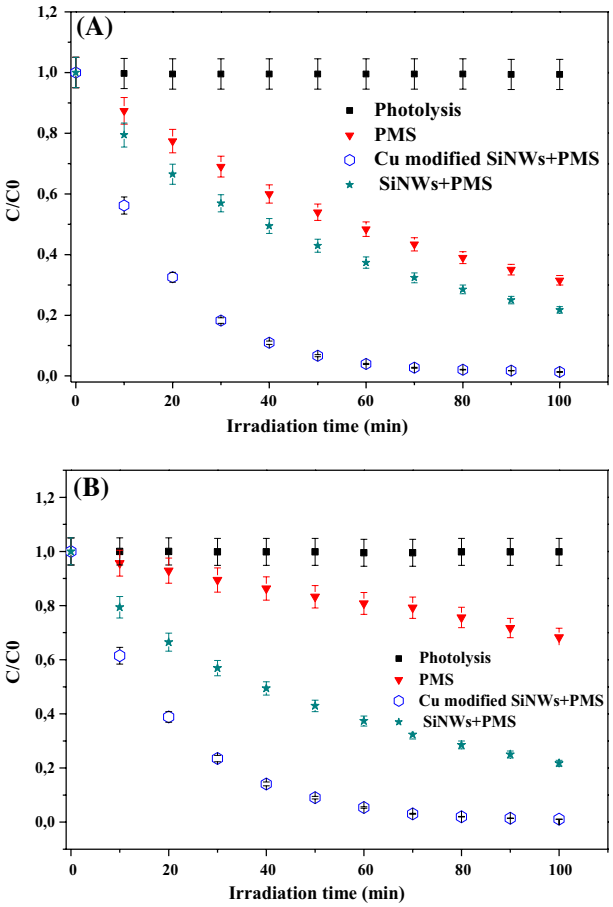

Fig. 5 Variation of MG degradation rate for different photocatalytic systems against time under; UV-light irradiations (**A**) and Visible light irradiations (**B**) ($C_0 = 2.5 \times 10^{-5}$ M, PMS = 0.3 mM, initial pH 6.1)

formation of p–n nanojunction between both p-type Cu2O and Cu phases, as identified by XRD analysis (Fig. 3B), and n-type SiNWs. This heterojunction prevents the recombination of the photogenerated electron–hole pairs thus improving the photocatalytic activity. It can be due also to the activation of PMS in the presence of SiNWs-Cu by one-electron reduction pathway in which PMS plays a role of radical precursor and electron acceptor, the electron source may be both the copper and water molecules [23, 46–48]. These results indicate that combining SiNWs-Cu with irradiation has synergistic effect on PMS activation, favoring MG photodegradation.

The difference between degradation rates under UV and visible light irradiations is due to the fact that Cu_2O has been known as a visible-light responsive photocatalyst [27].

The achieved degradation efficiency is better when compared to those reported by Yang et al. [2], Brahiti et al. [3] and Naama et al. [2, 3, 19], using modified SiNWs photocatalyst for the photodegradation of organic pollutants.

Mechanism and kinetic

Kinetic of degradation

The kinetic study of MG photodegradation was explored by taking the different initial concentration of MG in the range [1.5×10^{-5} – 1.25×10^{-4}] M (Fig. S4).

In order to determinate k_{app}, non-linear least square method was applied to photocatalytic data, the pseudo first order reaction kinetics is represented by Eq. 1 [49].

$$X = Ae^{-kapp.t} + E \tag{1}$$

Here

A is the amplitude of the process (M),

k_{app} is the pseudo-first order rate constant (min^{-1}),

t is the irradiation time (min),

E is the end point.

E is expected to be zero because the concentration of the reactant in a first order reaction tends to zero. In this process, the following linearization is possible [49]:

$$\ln X = \ln A - k_{app}\, t \tag{2}$$

To determine the constant parameters, nonlinear least-squares method was applied to the data of MG photodegradation using Origin 8.

The values of K_{app} and R^2 constants determined are listed in Table 1.

Results under UV (Fig. S4A) or visible (Fig. S4B) irradiation shows a possible description of the kinetic of photodegradation of MG by a pseudo first order model. The first order rate constants (K_{app}) are reported in Table 1 and results show that the degradation rate constant (K_{app}) increases with increasing the initial dye concentration especially for visible light irradiation which is accordant with the experimental results; more dye molecules are adsorbed on available active catalytic sites of SiNWs and donated more electrons to the conduction band of SiNWs. A better kinetic is observed with visible irradiation.

As can be seen in (Fig. S4), the reaction kinetics start to deviate slightly from those of pseudo-first order for the initial concentration of 0.125 mM and for both

Table 1 k_{app} and R^2 constants obtained by the non-linear least square fitting of the pseudo first order for MG photodegradation under UV and Visible light irradiations at different initial concentrations

Initial concentration (M)	Under UV irradiations		Under visible irradiations	
	R^2	k_{app} (min^{-1})	R^2	k_{app} (min^{-1})
1.5×10^{-5}	0.99	0.01 ± 0.001	0.99	$0.009\pm3.5\times10^{-4}$
2.5×10^{-5}	0.99	0.02 ± 0.001	0.99	0.04 ± 0.001
1.25×10^{-4}	0.90	0.062 ± 0.006	0.90	0.065 ± 0.006

Table 2 k_{app} and R^2 constants for pseudo-first and second-order reaction kinetics of MG dye photodegradation (0.125 mM) in the presence of Cu-modified SiNWs and PMS under UV and Visible light irradiations

Order	Under UV irradiations		Under visible irradiations	
	R^2	k_{app}/k_2 (min^{-1})	R^2	k_{app}/k_2 (min^{-1})
Pseudo-first	0.90	0.62 ± 0.006	0.90	0.65 ± 0.006
Second	0.79	76.6 ± 11.45	0.88	60.47 ± 6.48

irradiation types. In order to assess this deviation, we fitted the experimental data with pseudo first and second order kinetic models too. Table 2 show that the best fit was obtained using the pseudo-first order model with $R^2 = 0.90$ (Table 1) for both of UV and visible light irradiations.

In conclusion, the photocatalytic degradation of MG at the initial concentration of 0.125 mM is better described by the pseudo first-order kinetic model than by the others models.

The reaction kinetics of second order kinetic is described by the following equation:

$$\frac{1}{\mathrm{Ct}} = \frac{1}{C0} + K_2 \times \mathrm{t} \tag{3}$$

Here

C_0 represent the initial concentration of MG before irradiation (M),

C_t is the final concentration of MG after irradiation (M),

k_2 is the second order rate constant (min^{-1}) [38, 50, 51].

Table 3 shows a comparison of photodegradation efficiency of different photocatalysts based on SiNWs modified with metal nanoparticles reported in the literature with that of this work. It is clear that modified SiNWs elaborated in this work show a comparable performance.

Effect of MG configuration

The pH of MG solution was varied in the range 3.5–8 in order to examine the effect of ionization of MG molecule (Fig. S5). The pH value of MG solution was 6.1 and

Table 3 Photodegradation efficiency of different modified SiNWs

Modified SiNWs	Organic pollutant	Degradation rate (%)	k_{app} (min^{-1})	Irradiation type	Irradiation time (min)	References
Cu_2O—SiNWs	Rhodamine B	97.5	0.0611	Visible	60	[2]
Au- SiNWs	Methylene blue	91.93	–	UV	200	[3]
Cu-SiNWs	Tartrazine	95.48	–	UV	200	[19]
Cu-SiNWs	Malachite green	98.69	0.02 ± 0.001	UV	100	This work
Cu-SiNWs	Malachite green	99	0.04 ± 0.006	Visible	100	This work

was adjusted using few drops of HCl or NaOH solutions. As shown in (Fig. S5), pH has a significant effect on the photodegradation rate increases with increasing the pH regardless the type of irradiation. Importantly, the optimal solution pH was observed at pH 6.1.

These results are explained by the fact that the adsorption of MG molecules (pKa = 10) on the sites of the catalyst is depends on its surface charge. Indeed, at $pH < pH_{pzc,}$ the SiNWs surface sites are positively charged which decreases the active surface sites available for adsorption. On the other hand and at $pH > pH_{pzc,}$ the SiNWs sites become negative thus, causing an intensification of the adsorption of the cationic species of the MG dye.

Degradation mechanism of MG

The high photocatalytic performance of SiNWs-Cu heterojunctions can be due to the formation of p–n junction between p-type Cu2O nanoparticles and n-type SiNWs.

The mechanism using SiNWs-Cu in the photodegradation of organic dye is generally known as follows: After absorption of light photons with an energy equal to or greater than the bands gaps of SiNWs and Cu_2O nanoparticles, electrons are excited from VB to CB, then the electrons transfer from the CB of Cu_2O to that of SiNWs, leaving holes in the VB of Cu_2O, in the other side the holes of SiNWs are transferred to the VB of Cu_2O causing the formation and the separation of electron–hole ($e-/h^+$) (Eqs. 4, 5 and 6).

The photo-generated holes can immediately attack malachite green dye molecules, while photo-generated electrons react with absorbed O_2 on the surface of SiNWs or dissolved O_2 in water to form superoxide ion radicals ($O_2^{\cdot}$) which can degrade MG dye molecules. (Eq. 7) Afterwards $O_2^{\cdot}$ radicals react with H^+ to generate $HO_2^{\cdot}$ and $OH^{\cdot}$ radicals.

Under such conditions, malachite green species in suspension react with adsorbed water and $OH^{\cdot}$ radicals which are effective oxidizing agents and non selective towards organic pollutants. The MG molecules can be oxidized and decomposed by $OH^{\cdot}$ radicals (Eq. 8) [2, 3, 19].

$$\mathrm{SiNWs} + \mathrm{hv} \geq \mathrm{E_g} \rightarrow \mathrm{e^-_{CB}} + \mathrm{h^+_{VB}} \tag{4}$$

$$\mathrm{h^+_{VB}} + \mathrm{OH^-} \rightarrow \mathrm{OH^{\cdot}} \tag{5}$$

$$\mathrm{h^+_{VB}} + \mathrm{H_2O} \rightarrow \mathrm{OH^{\cdot}} + \mathrm{H^+} \tag{6}$$

$$\mathrm{e-} + \mathrm{O_2} \rightarrow \mathrm{O_2^{\cdot}} \tag{7}$$

$$\mathrm{OH^{\cdot}} + \mathrm{MG} \rightarrow \mathrm{Intermediates} \rightarrow \mathrm{CO_2} + \mathrm{H_2O} \tag{8}$$

The mineralization of MG was investigated by total organic carbon measurement after UV and visible irradiations. A high reduction of carbon values in the solution

Table 4 TOC values of MG dye solution before and after photodegradation reaction under UV and Visible light irradiations

	Before irradiation TOC (ppm)	After irradiation TOC (ppm)	Photodegradation Efficiency (%)
Under UV irradiations	18.04	0.86	98.69
Under visible irradiations	18.11	0.87	99

(99%) confirming the mineralization of MG (Table 4), which is in good agreement with our results presented on figures (Fig. 5) and (Fig. S3).

Stability of SiNWs material

To study the durability and the reusability of SiNWs-Cu, photocatalysis experiments were conducted four times. After each use, the catalytic material was rinsed and dried. The MG concentration was kept the same for each experiment. The photocatalyst were used several times without notable loss of its efficiency. As shown in (Fig. S6), the activity of SiNWs-Cu is stable with a constant degradation efficiency of 99% of MG in 100 min up to 3rd cycle, but starts to lose its performance after 4th successive cycles of degradation tests.

These results indicate that SiNWs-Cu exhibits an effective and stable photocatalytic performance and could be successfully reused for 4 successive cycles without any significant change of its activity.

Conclusion

Silicon nanowires array were elaborated by one-step metal-assisted chemical etching of silicon substrate in aqueous HF/$AgNO_3$ solution and modified with Cu nanoparticles by an electroless deposition process.

The structure, the morphology and the chemical composition of prepared samples was studied using XRD, SEM, EDS and FTIR techniques.

Cu-modified SiNWs were used as heterogeneous photocatalyst for the photodegradation of malachite green MG (2.5×10^{-5} M) under UV and visible light irradiations. The results show that SiNWs-Cu present higher photocatalytic activity (98.69 and 99% for UV and visible light irradiation, respectively) than unmodified SiNWs (78.23 and 78.4% for UV and visible light irradiation, respectively), which was ascribed to the formation of nano-heterojunction between Cu_2O nanoparticles and SiNWs preventing the rapid recombination of photogenerated electron–hole pairs. An important enhancement of photodegradation process was noted when a very low amount of PMS was added to the MG solution, Indeed, total mineralization of MG was achieved after 100 min of UV/Visible irradiations. The stability of Cu-SiNWs was approved through cyclic experiments which demonstrate its constant photocatalytic performance. According to the obtained results we can conclude that

SiNWs-Cu may have notable interest for organic waste treatment and sustainable development.

Supplementary Information The online version contains supplementary material available at https://doi.org/10.1007/s11144-021-02106-5.

Acknowledgements The authors gratefully acknowledge the financial support from General Direction of Scientific Research and of Technological Development of Algeria (DGRSDT/MESRS) in collaboration with university of Limoges (PEIRENE EA7500).

References

1. Amdouni S, Cherifi Y, Coffinier Y, Addad A, Zaïbi MA, Oueslati M, Boukherroub R (2018) Gold nanoparticles coated silicon nanowires for efficient catalytic and photocatalytic applications. Mater Sci Semicond Process 75:206–213
2. Yang C, Wang J, Mei L, Wang X (2014) Enhanced photocatalytic degradation of rhodamine B by Cu_2O coated silicon nanowire arrays in presence of H_2O_2. J Mater Sci Technol. https://doi.org/10.1016/j.jmst.2014.03.023
3. Brahiti N, Hadjersi T, Menari H, Amirouche S, El Kechai O (2015) Enhanced photocatalytic degradation of methylene blue by metal-modified silicon nanowires. Mater Res Bull 62:30–36
4. Gonchar KA, Agafilushkina SN, Moiseev DV, Bozhev IV, Manykin AA, Kropotkina EA, Gambaryan AS, Osminkina LA (2020) H1N1 influenza virus interaction with a porous layer of silicon nanowires. Mater Res Express. https://doi.org/10.1088/2053-1591/ab7719
5. Hamdi A, Boussekey L, Roussel P, Addad A, Ezzaouia H, Boukherroub R, Coffinier Y (2016) Hydrothermal preparation of MoS_2/TiO_2/Si nanowires composite with enhanced photocatalytic performance under visible light. Mater Des. https://doi.org/10.1016/j.matdes.2016.07.098
6. Lian S, Tsang CHA, Kang Z, Wong N, Lee ST (2011) Hydrogen-terminated silicon nanowire photocatalysis: benzene oxidation and methyl red decomposition. Mater Res Bull 46:2441–2444
7. Megouda N, Hadjersi T, Coffinier Y, Szunerits S, Boukherroub R (2016) Investigation of morphology, reflectance and photocatalytic activity of nanostructured silicon surfaces. Microelectron Eng 159:94–101
8. Casiello M, Picca RA, Fusco C, D'Accolti L, Leonardi AA, Lo Faro MJ, Irrera A, Trusso S, Cotugno P, Sportelli MC, Cioffi N (2018) Catalytic activity of silicon nanowires decorated with gold and copper nanoparticles deposited by pulsed laser ablation. Nanomaterials 8:78
9. Karthikeyan C, Arunachalam P, Ramachandran K, Al-Mayouf AM, Karuppuchamy S (2020) Recent advances in semiconductor metal oxides with enhanced methods for solar photocatalytic applications. J Alloys Compd. https://doi.org/10.1016/j.jallcom.2020.154281
10. Kolay A, Maity D, Ghosal P, Deepa M (2019) Selenium nanoparticles decorated silicon nanowires with enhanced liquid junction photoelectrochemical solar cell performance. J Phys Chem light. https://doi.org/10.1021/acs.jpcc.9b00062
11. Mokshin PV, Juneja S, Pavelyev VS (2019) Synthesis of silicon nanowires using plasma chemical etching process for solar cell applications. J Phys Conf Ser 1368:022060
12. Abdulkadir A, Abdul Aziz A, Zamir Pakhurudin M (2020) Effects of silver nanoparticles layer thickness towards properties of black silicon fabricated by metal assisted chemical etching for photovoltaics. SN Appl Sci 2:1–8
13. Markose KK, Shaji M, Bhatia S, Nair P, Saji KJ, Antony A, Jayara MK (2020) Novel boron doped p-type Cu_2O thin film as hole selective contact in c-Si solar cell. Appl Mater Interfaces. https://doi.org/10.1021/acsami.9b22581
14. Su DS, Chen PY, Chiu HC, Han CC, Yen TJ, Chen HM (2019) Disease antigens detection by silicon nanowires with the efficiency optimization of their antibodies on a chip. Biosens Bioelectron 141:111209
15. Ghosh R, Ghosh J, Das R, Mawlong LPL, Paul K, Gir PK (2018) Multifunctional Ag nanoparticle decorated Si nanowires for sensing photocatalysis and light emission applications. J Colloid Interface Sci. https://doi.org/10.1016/j.jcis.2018.07.123

16. Huang Z, Chen S, Wang Y, Li T (2020) Gold nanoparticle modified silicon nanowire array based sensor for lowcost, high sensitivity and selectivity detection of mercury ions. Mater Res Express 7:035017
17. Wang F, Deng Y, Yuan C (2019) Comparative life cycle assessment of silicon nanowire and silicon nanotube based lithium ion batteries for electric vehicles. Procedia CIRP 80:310–315
18. Gao A, Chen S, Wang Y, Lie T (2018) Silicon nanowire field-effect-transistor-based biosensor for biomedical applications. Sens Mater 30:1619–1628
19. Naama S, Hadjersi T, Menari H, Nezzal G, Baba Ahmed L, Lamrani S (2016) Enhancement of the tartrazine photodegradation by modification of silicon nanowires with metal nanoparticles. Mater Res Bull 76:317–326
20. Yu Y, Zhao Y, Sun H, Ahmad M (2013) Au nanoparticles decorated CuO nanowire arrays with enhanced photocatalytic properties. Mater Lett 108:41–45
21. Pan K, Ming H, Yu H, Huang H, Liu Y, Kang Z (2012) Copper nanoparticles modified silicon nanowires with enhanced cross-coupling catalytic ability. Dalton Trans 41:2564–2566
22. Xiong Z, Zheng M, Li H, Ma L, Shen W (2013) Fabrication and optical properties of silicon nanowire /Cu_2O nano heterojunctions by electroless deposition technique. Mater Lett 112:211–214
23. Kangralkar MV, Kangralkar VA, Momin N, Manjanna J (2019) Cu_2O nanoparticles for adsorption and photocatalytic degradation of methylene blue dye from aqueous medium. Environ Nanotechnol Monit Manag 12:100265
24. Hu Y, Luo Y, Liu S, Zhang RS, Wang F, Li Y, Li S, Zhong W (2020) Fabrication of Cu_2O/Si nanowires photocathode and its photoelectrochemical properties. Semicond Sci Technol. https://doi.org/10.1088/1361-6641/ab73e8
25. Moulai F, Hadjersi T, Ifires M, Khen A, Rachedi N (2019) Enhancement of electrochemical capacitance of silicon nanowires arrays (SiNWs) by modification with manganese dioxide MnO_2. SILICON. https://doi.org/10.1007/s12633-019-0066-7
26. Tao B, Miao F, Chu PK (2015) Fabrication and photoelectrochemical study of vertically oriented TiO_2/Ag/SiNWs arrays. J Alloys Compd 635:112–117
27. Kakutaa S, Abe T (2009) Photocatalytic activity of Cu_2O nanoparticles prepared through novel synthesis method of precursor reduction in the presence of thiosulfate. Solid State Sci 11:1465–1469
28. He Q, Liu J, Tian Y, Wu Y, Magesa F, Deng P, Li G (2019) Facile preparation of Cu_2O nanoparticles and reduced graphene oxide nanocomposite for electrochemical sensing of rhodamine B. Nanomaterials 9:958
29. Zhang Y, Zeng W, Li Y (2019) Porous MoS_2 microspheres decorated with Cu_2O nanoparticles for ammonia sensing property. Mater Lett 241:223–226
30. Cong DS, Hai PN, Bang N (2017) Synthesis and optical properties of Cu_2O and Au-Cu_2O core-shell particles. J Sci Math Phys 33:73–79
31. Sathiya SM, Okram GS, Jothi M (2017) Structural, optical and electrical properties of copper oxide nanoparticles prepared through microwave assistance. Adv Mater Proc 2:371–377
32. Chatterjee S, Saha SK, Pal AJ (2016) Formation of all-oxide solar cells in atmospheric condition based on Cu_2O thin-films grown through SILAR technique. Sol Energy Mater Sol Cells 147:17–26
33. Bhavyasree PG, Xavier TS (2020) Green synthesis of Copper Oxide/Carbon nanocomposites using the leaf extract of AdhatodavasicaNees, their characterization and antimicrobial activity. Heliyon 6:e03323
34. Khalaji AD, Jarosova M, Machek P (2020) The Preparation, structural characterization, optical properties, and antibacterial activity of the CuO/Cu_2O nanocomposites prepared by the facile thermal decomposition of a new copper precursor. Nanomed J 7:231
35. Lavand AB, Bhatub MN, Malghe YS (2018) Visible light photocatalytic degradation of malachite green using modified Titania. J Mater Res Technol. https://doi.org/10.1016/j.jmrt.2017.05.019
36. Rabie AM, Abukhadra MR, Rady AM, Ahmed SA, Labena A, Mohamed HSH, Betiha MA, Shim JJ (2020) Instantaneous photocatalytic degradation of malachite green dye under visible light using novel green Co–ZnO/ algae composites. Res Chem Intermed. https://doi.org/10.1007/s11164-019-04074-x
37. Arsalani N, Bazazi S, Abuali M, Jodeyri S (2019) A new method for preparing ZnO/CNT nanocomposites with enhanced photocatalytic degradation of malachite green under visible light. J Photochem Photobiol A Chem. https://doi.org/10.1016/j.jphotochem.2019.112207
38. Mark JA, Venkatachalam A, Pramothkumar A, Senthilkumar N, Jothivenkatachalam K, Prince Jesuraj J (2020) Investigation on structural, optical and photocatalytic activity of $CoMn_2O_4$ nanoparticles

prepared via simple co-precipitation method. Phys B Phys Condens Matter. https://doi.org/10.1016/j.physb.2020.412349
39. Hasan I, Bhatia D, Walia S, Singh P (2020) Removal of malachite green by polyacrylamide-g-chitosan γ-Fe_2O_3 nanocomposite an application of central composite design. Singh Groundw Sustain Dev. https://doi.org/10.1016/j.gsd.2020.100378
40. Saad AM, Abukhadra MR, Abdel-Kader AS, Elzanaty Al M, Mady AH, Betiha MA, Shim JJ, Rabie AM (2020) Photocatalytic degradation of malachite green dye using chitosan supported ZnO and Ce–ZnO nano-flowers under visible light. J Environ Manage 258:110043
41. Solis-Casados A, Martinez-Pena J, Hernandez-Lopez S, Escobar-Alarcon L (2020) Photocatalytic degradation of the malachite green dye with simulated solar light using TiO_2 modified with Sn and Eu. Top Catal. https://doi.org/10.1007/s11244-020-01240-z
42. Hakimyfard A, Tahmasebi N, Samimifar M, Naghizadeh M (2020) Pure and Gd^{3+}, Tb^{3+} and Ho^{3+}-doped $As_2Ni_3O_8$: a new visible light induced photocatalyst for the photodegradation of malachite green water pollutant. J Nanostruct 10:9–19
43. Das CK, Dhar SS (2020) Rapid catalytic degradation of malachite green by $MgFe_2O_4$ nanoparticles in presence of H_2O_2. J Alloys Compd 828:154462
44. Surendra BS, Shekhar TRS, Veerabhadraswamy M, Nagaswarupa HP, Prashantha SC, Geethanjali GC, Likitha C (2020) Probe sonication synthesis of $ZnFe_2O_4$ NPs for the photocatalytic degradation of dyes and effect of treated wastewater on growth of plants. Chem Phys Lett. https://doi.org/10.1016/j.cplett.2020.137286
45. Mohameda A, Ghobaraa MM, Abdelmaksoud MK, Mohamed GG (2019) A novel and highly efficient photocatalytic degradation of malachite green dye via surface modified polyacrylonitrile nanofibers/biogenic silica composite nanofibers. Sep Purif Technol 210:935–942
46. Chi H, Wang Z, He X, Zhang J, Wang D, Ma J (2019) Activation of peroxymonosulfate system by copper-based catalyst for degradation of naproxen. Mech Pathw Chemosphere 228:54–64
47. Cao J, Lai L, Lai B, Yao G, Chen X, Song L (2019) Degradation of tetracycline by peroxymonosulfate activated with zerovalentiron: Performance, intermediates, toxicity and mechanism. Chem Eng J 364:45–56
48. Ahna Y-Y, Baeb H, Kimc H-I, Kimd S-H, Kime J-H, Leef S-G, Leea J (2019) Surface-loaded metal nanoparticles for peroxymonosulfate activation: Efficiency and mechanism reconnaissance. Appl Catal B: Environ 241:561–569
49. Lente G (2018) Facts and alternative facts in chemical kinetics: remarks about the kinetic use of activities, termolecular processes, and linearization techniques. Curr Opin Chem Eng 21:76–83
50. Abukhadra MR, Shaban M, Abd El Samad MA (2018) Enhanced photocatalytic removal of Safranin-T dye under sunlight within minute time intervals using heulandite/polyaniline@ nickel oxide composite as a novel photocatalyst. Ecotoxicol Environ Saf 162:261–271
51. Mohamed F, Abukhadra MR, Shaban M (2018) Removal of Safranin dye from water using polypyrrole nanofiber/Zn-Fe layered double hydroxide nanocomposite (Ppy NF/Zn-Fe LDH) of enhanced adsorption and photocatalytic properties. Sci Total Environ 640:352–363